Galaxies and Extragalactic Astronomy

12. Semi-Analytical Models of galaxy formation

2. SAMs of Galaxy Formation

2.1 Introduction

- Two stages:
  - Dark Matter structure formation
  - Galaxies: baryons cool and collapse to DM potential wells
- Dark Matter interacts only through gravity. Evolution of dark matter halos understood with numerical simulations
- Evolution of galaxies is a complex process
- two main ways to study it: Semi-analytical models and hydrodynamic simulations

2. SAMs of Galaxy Formation

2.2 History

- White & Rees 1978
- More detail: Cole (1991), White & Frenk (1991), Lacey & Silk (1991)
- merging and hierarchical formation: Kauffmann et al (1993) & Cole et al (1994)
- Other groups developed codes with different levels of sophistication since the late 90s

2. SAMs of Galaxy Formation

2.3 Main Codes

- Galform (Durham): Lacey et al 2016
- Munich: LGalaxies (Henriques et al 2013), SAGE (Croton et al 2006), DLB07 (De Lucia & Blaizot 2007)
- Galacticus: Benson 2012
- GalICS: Cattaneo et al
- MORGANA: Monaco et al 2007
- SAG: Gargiulo et al 2014
- SantaCruz: Somerville et al 2008
- YSAM: Lee & Yee 2013

2. SAMs of Galaxy Formation

2.3 Basic Ingredients

- Cosmological model
  - ΛCDM
  - initial condition fluctuations are Gaussian
- Dark Matter halos: concentrations of DM where galaxies are formed
  - abundance of DM halos (halo MF)
  - assembly of DM halos (merger trees)
  - structure of DM halos (NFW, angular momentum,…)

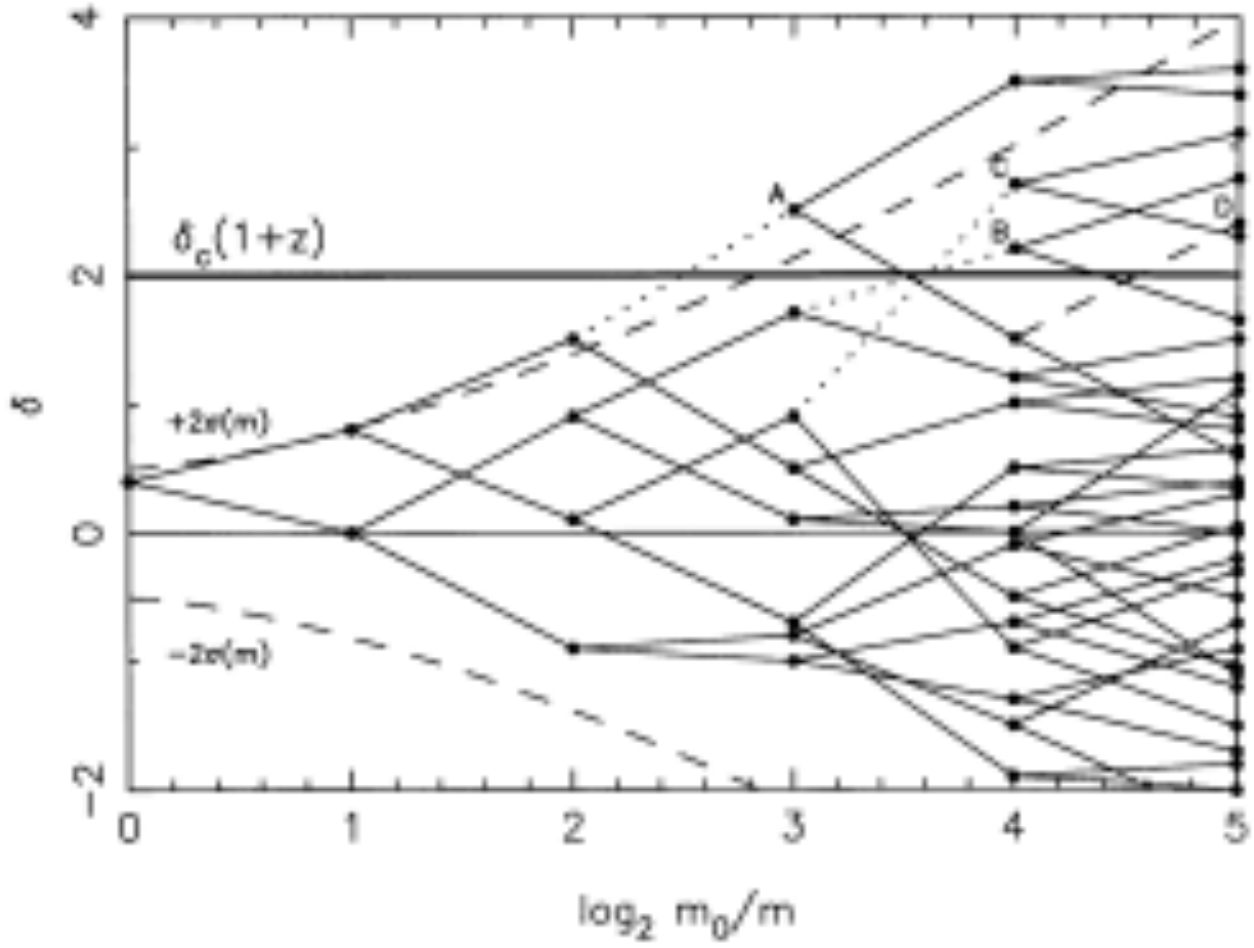

Block Model

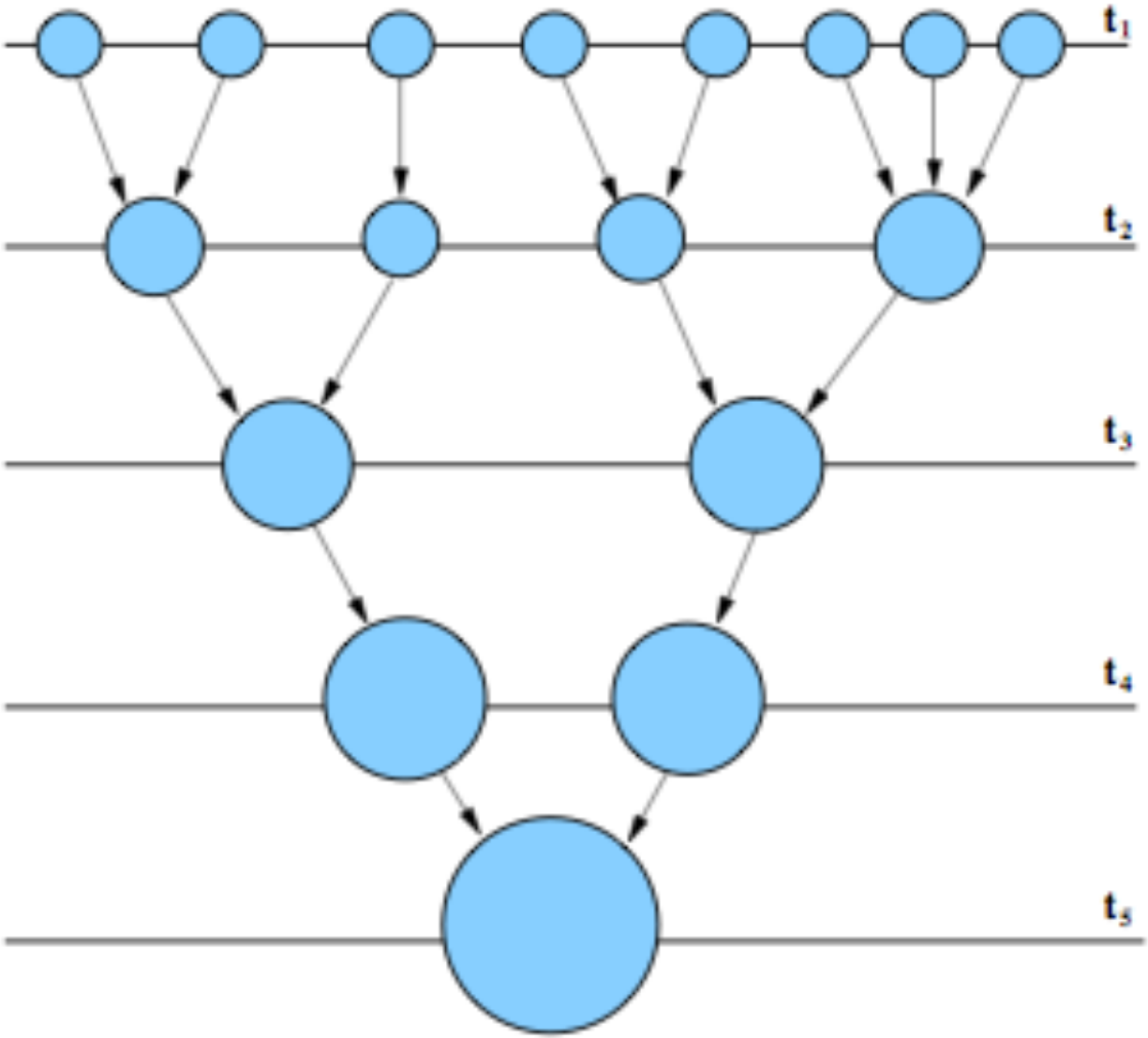

Halo merger tree

Halo merger tree

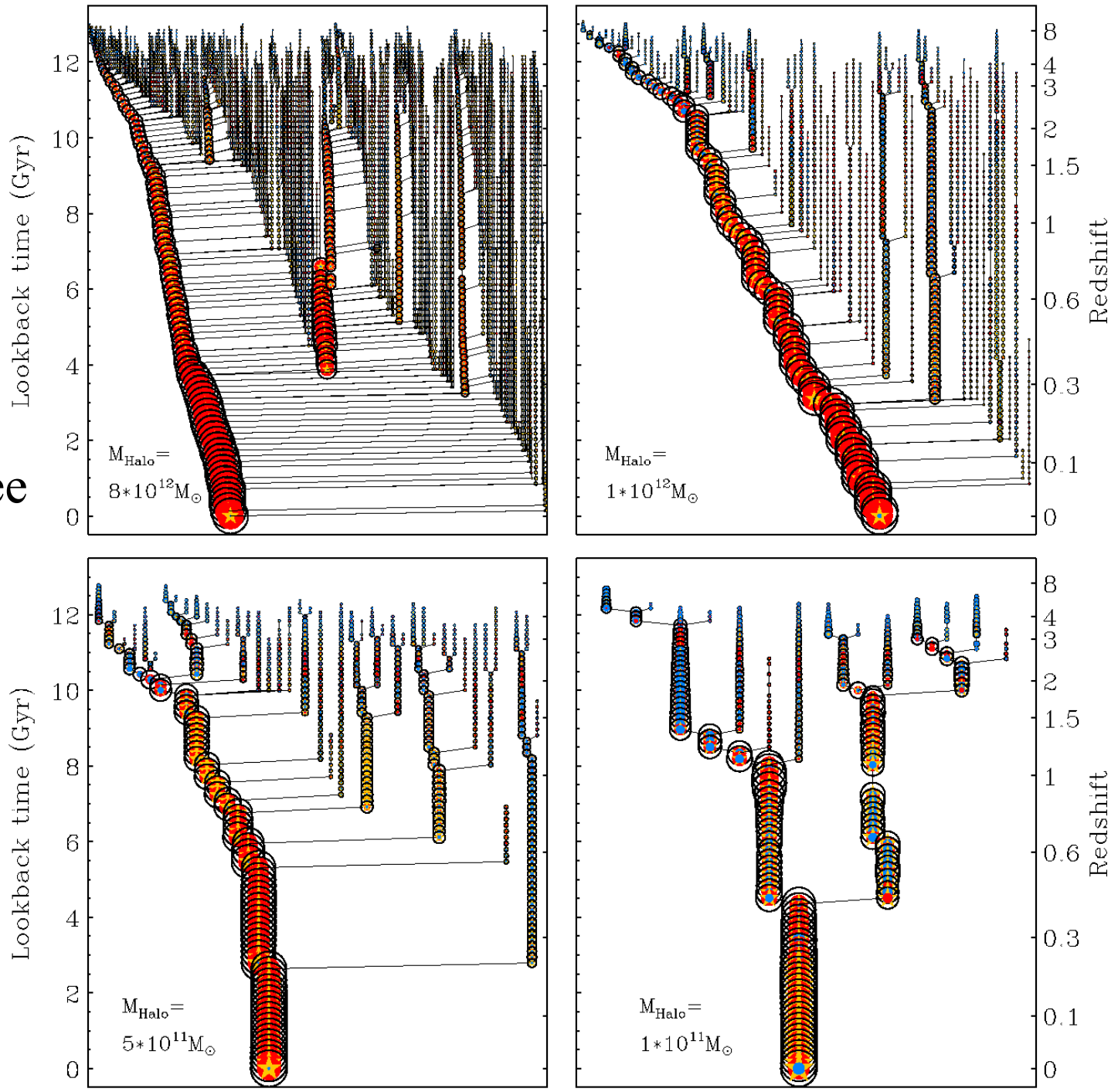

2. SAMs of Galaxy Formation

2.3 Basic Ingredients

- Gas cooling
- Star Formation
- Feedback processes
- Chemical evolution
- Galaxy mergers
- Galaxy sizes
- Spectral energy distribution
- Black Hole growth

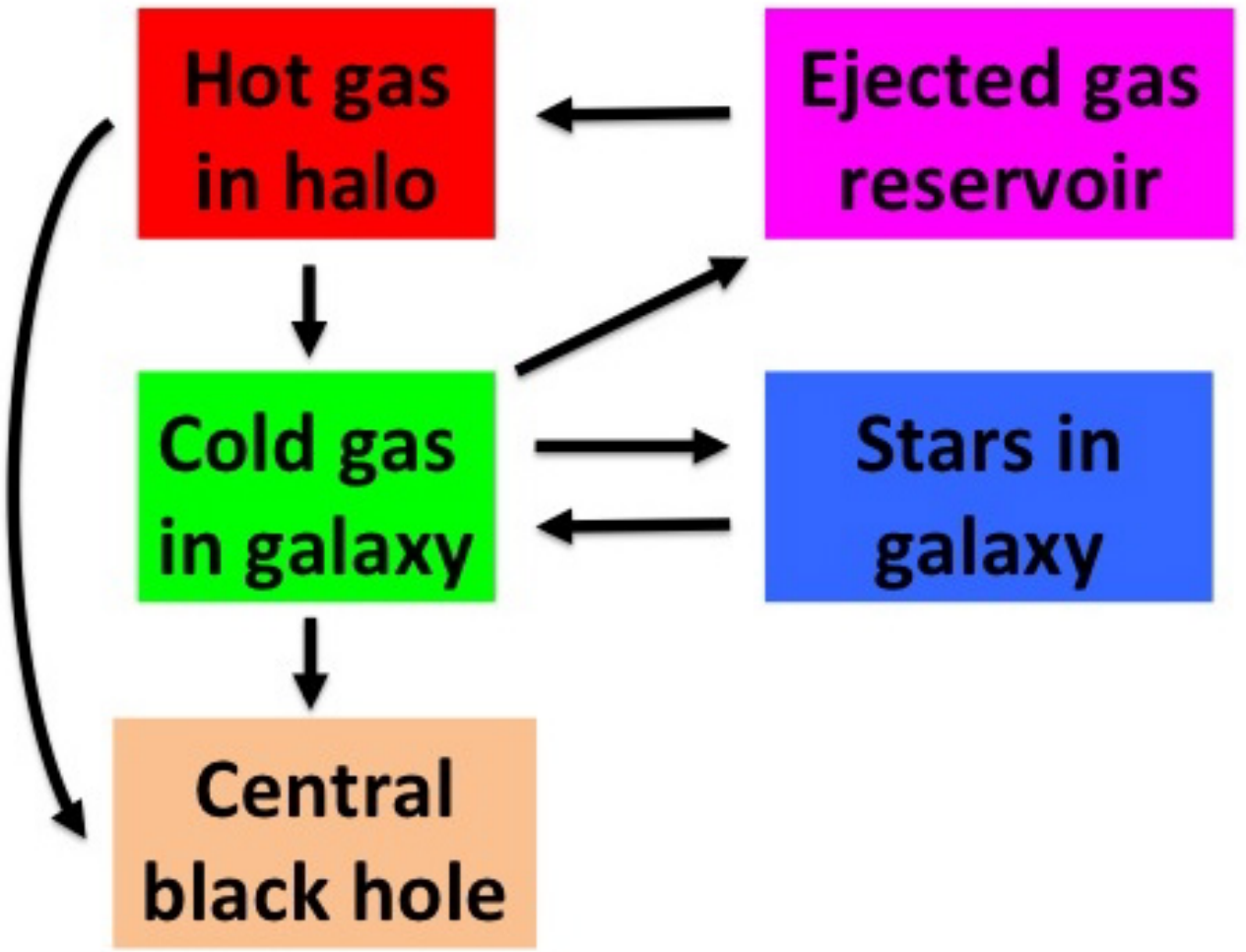
Hot gas in halo
Ejected gas reservoir
Cold gas in galaxy
Stars in galaxy
Central black hole

Components

SAM recipe

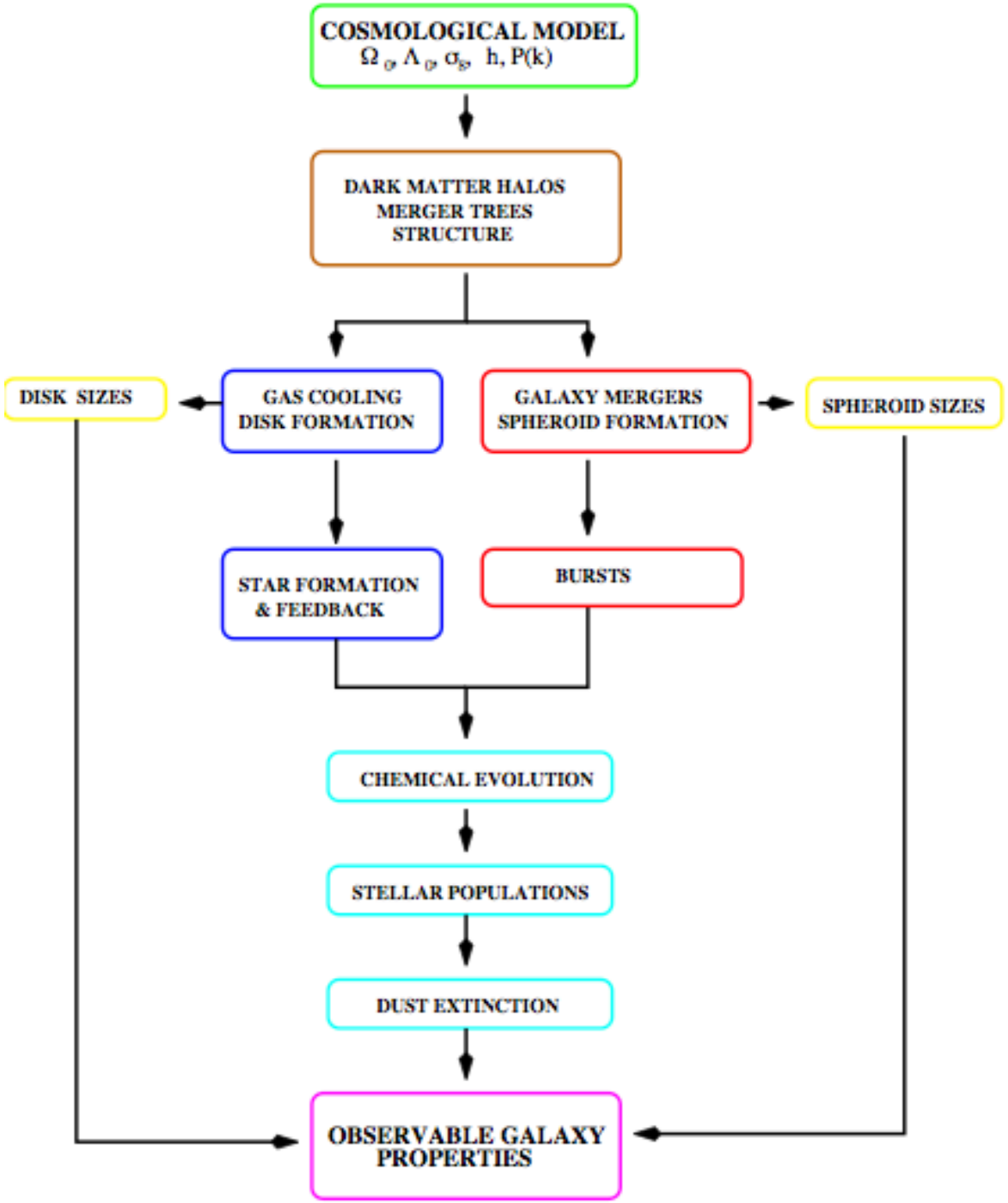
COSMOLOGICAL MODEL
$\Omega_0, \Lambda_0, \sigma_8$, h, P(k)
DARK MATTER HALOS
MERGER TREES
STRUCTURE
DISK SIZES
GAS COOLING
DISK FORMATION
GALAXY MERGERS
SPHEROID FORMATION
SPHEROID SIZES
STAR FORMATION
& FEEDBACK
BURSTS
CHEMICAL EVOLUTION
STELLAR POPULATIONS
DUST EXTINCTION
OBSERVABLE GALAXY
PROPERTIES

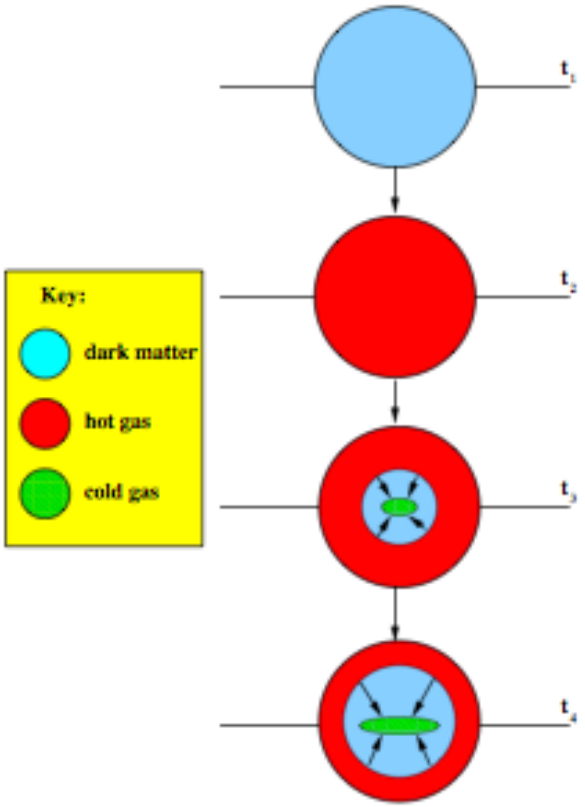

Figure 8. A schematic of the basic cooling model used in semi-analytical models. Each line represents a stage in the cooling process. In the first step (t_1), baryons fall into the gravitational potential well of the dark matter halo. The presence of a photo-ionising background may reduce the fraction of baryons that fall into low mass haloes, as described in the text. This gas is assumed to be heated by shocks as it falls into the potential well, attaining the virial temperature associated with the halo (t_2). In the third step (t_3), the inner parts of the hot gas halo cool, forming a rotationally supported disc. At a later stage (t_4), the radius within which gas has had time to cool advances outwards towards the virial radius of the halo and the cold gas disc grows in size.

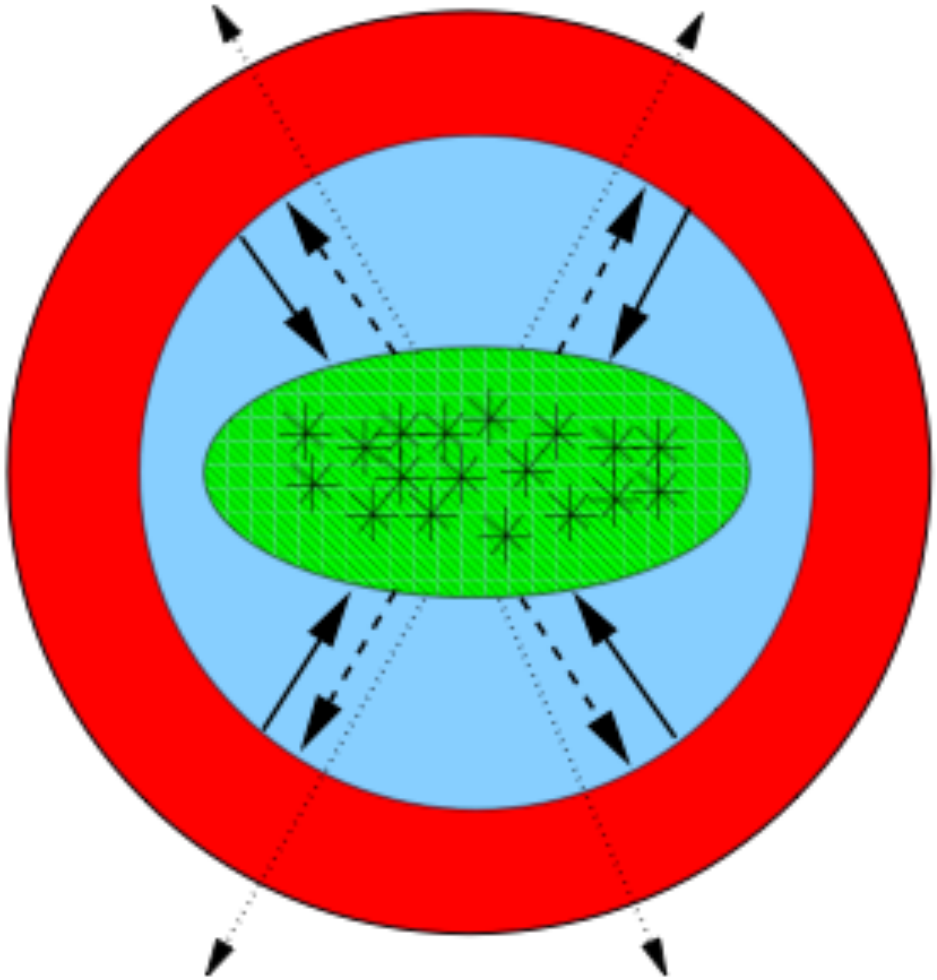

Processes in a halo

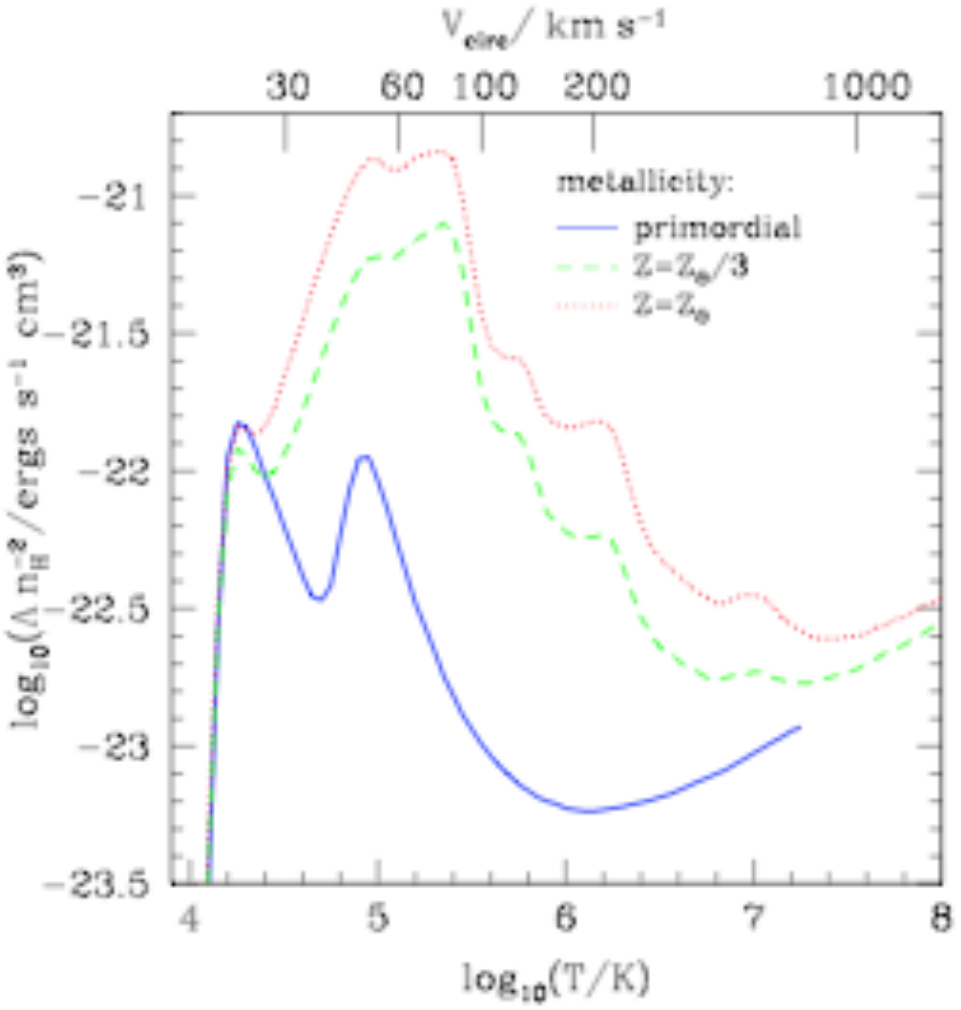

Cooling rate

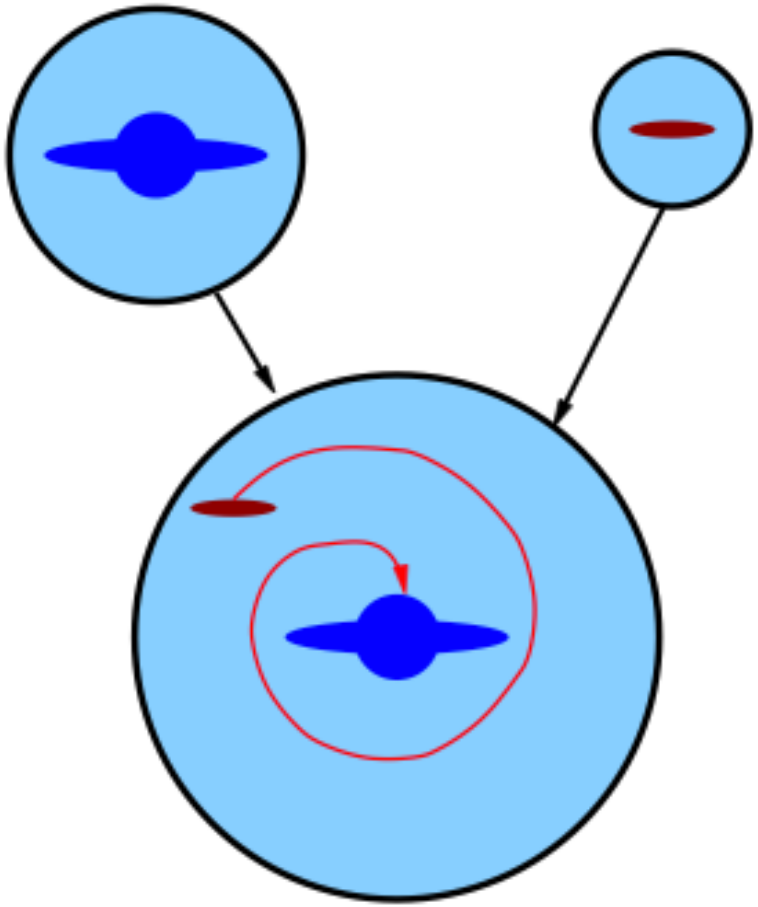

Merging halos

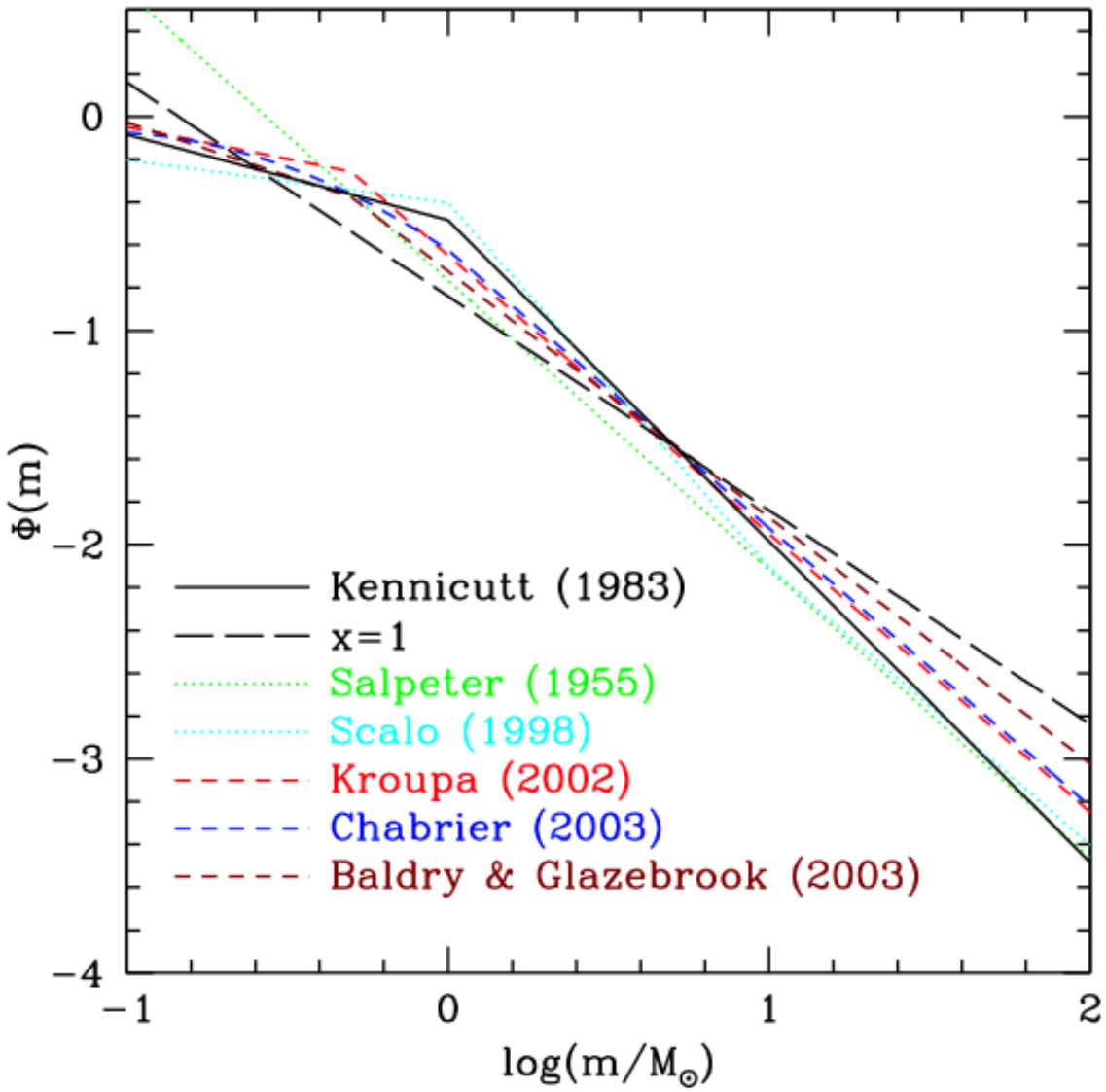

Initial Mass Function

GALFORM parameters

parameter	value	range	type=F/P/S	description	Eqn/paper
Cosmology				Komatsu et al. (2011)	
Ω_{m0}	0.272	-	F	matter density	
Ω_{b0}	0.0455	-	F	baryon density	
h	0.704	-	F	Hubble parameter	
σ_8	0.81	-	F	fluctuation amplitude	
n_s	0.967	-	F	scalar spectral index	
Stellar population					Maraston (2005)
IMF : quiescent					
x	Kennicutt	-	F	IMF	Eqn. 32
p	0.021	-	F	yield	Eqn. 31
R	0.44	-	F	recyled fraction	Eqn. 30
IMF : starburst					
x	1	0-1	P	IMF slope	Eqn. 32
p	0.048	-	P	yield	Eqn. 31
R	0.54	-	P	recyled fraction	Eqn. 30
Star formation: quiescent					Lagos et al. (2011b)
ν_{SF}	0.74 Gyr^{-1}	0.25 – 0.74 Gyr^{-1}	P	efficiency factor for molecular gas	Eqn. 7
P_0	1.7×10^4	-	F	normalisation of pressure relation	Eqn. 6
α_P	0.8	-	F	slope of pressure relation	Eqn. 6
Star formation: bursts					Baugh et al. (2005)
f_{dyn}	20	0 - 100	P	multiplier for dynamical time	Eqn. 9
$\tau_{*burst,min}$	0.1 Gyr	0-1.0	P	minimum burst timescale	Eqn. 9
Photoionization feedback					Benson et al. (2003)
z_{reion}	10	-	F	reionization redshift	
V_{crit}	30 $km\,s^{-1}$	-	F	threshold circular velocity	
SNe feedback					Cole et al. (2000)
V_{SN}	320 $km\,s^{-1}$	anything	P	pivot velocity	Eqn. 10
γ_{SN}	3.2	0-5.5	P	slope on velocity scaling	Eqn. 10
α_{ret}	0.64	0.3-3	P	reincorporation timescale multiplier	Eqn. 11
AGN feedback & SMBH growth					Bower et al. (2006)
f_{BH}	0.005	0.001-0.01	S	fraction of mass accreted onto BH in starburst	Malbon et al. (2007)
α_{cool}	0.8	0-2	P	ratio of cooling/free-fall time	Eqn. 12
f_{Edd}	0.01	-	S	controls maximum BH heating rate	Eqn. 13
ϵ_{heat}	0.02	-	S	BH heating efficiency	
Disk stability					Cole et al. (2000)
F_{stab}	0.9	0.9-1.1	P	threshold for instability	Eqn. 15
Galaxy mergers					Jiang et al. (2008)
Size of merger remnants					Cole et al. (2000)
f_{orbit}	0	0 - 1	S	orbital energy contribution	Eqn. 19
f_{DM}	2	-	S	dark matter fraction in galaxy mergers	
Starburst triggering in mergers					Baugh et al. (2005)
f_{ellip}	0.3	0.2 - 0.5	P	threshold on mass ratio for major merger	
f_{burst}	0.05	0.05 - 0.3	S	threshold on mass ratio for burst	
Dust model					Granato et al. (2000)
f_{cloud}	0.5	0.2 - 0.8	P	fraction of dust in clouds	
t_{esc}	1 Myr	1 – 10 Myr	P	escape time of stars from clouds	Eqn. A5
β_b	1.5	1.5 - 2	S	sub-mm emissivity slope in starbursts	Eqn. 38

Note: P_0 in units $k_B cm^{-3} K$

Effect of changing parameters in GALFORM

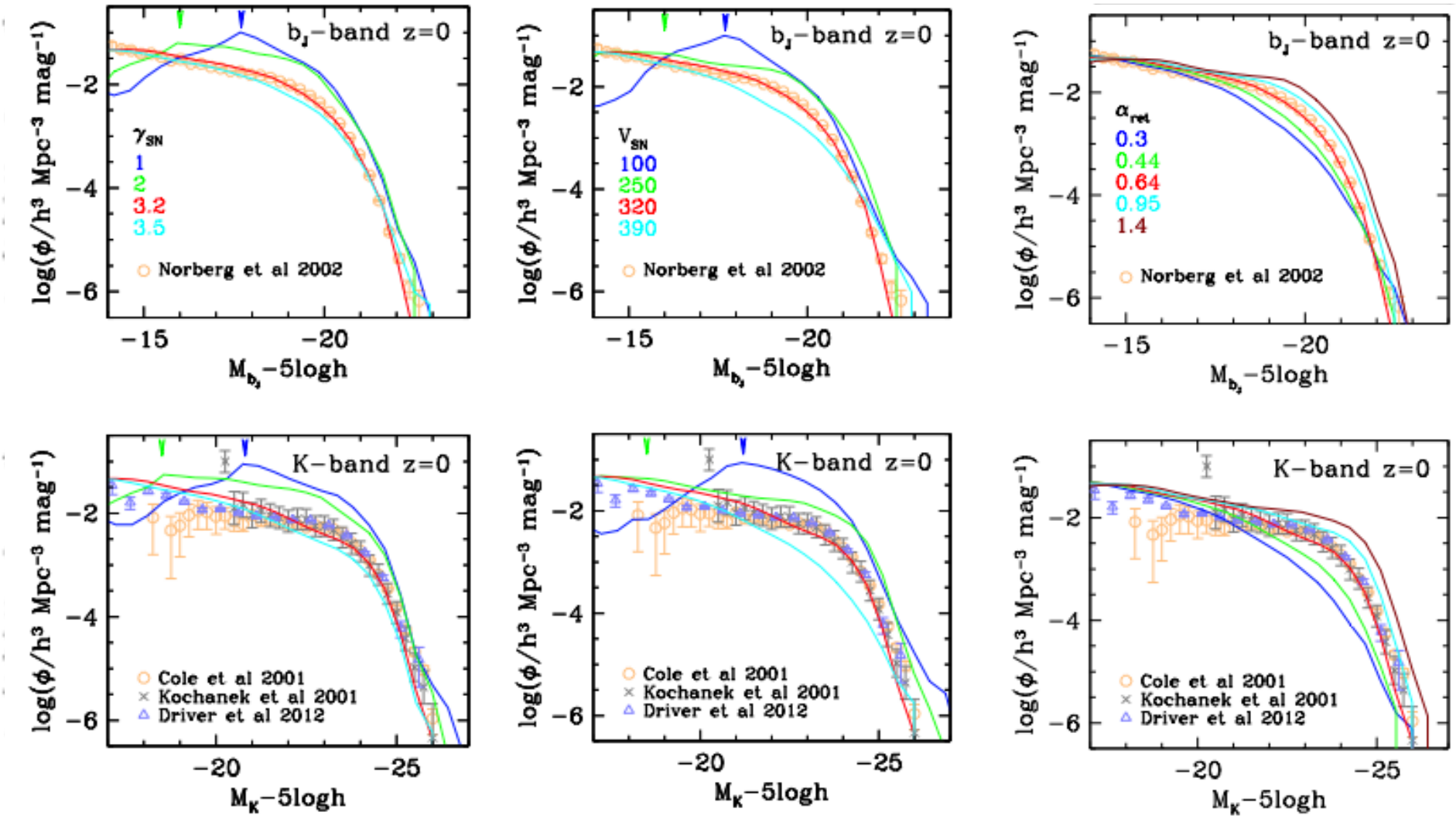

Figure C1. Effects on the b_J- and K-band LFs at $z = 0$ of varying the supernova feedback parameters $\gamma_{\rm SN}$ and $V_{\rm SN}$ (left and middle columns) and the gas return parameter $\alpha_{\rm ret}$ (right column). Only one parameter is varied in each column, and the values are given in the key in each panel, with the red curve showing the standard model in all cases. The vertical arrows at the top of each panel indicate the luminosity below which the results for the corresponding model are affected by the halo mass resolution. The observational data plotted are the same as in Fig. 3.

Effect of changing parameters in GALFORM

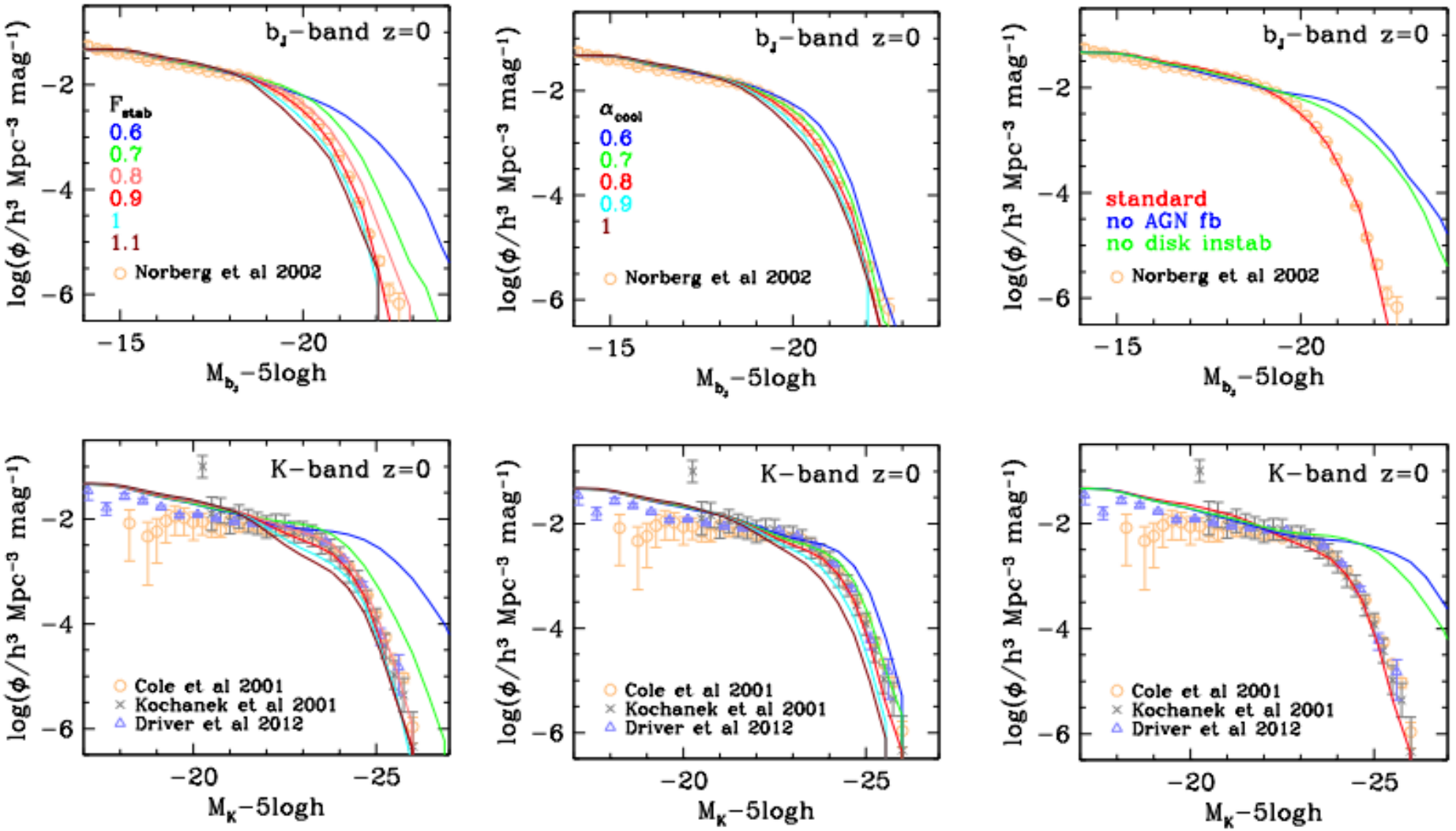

Figure C2. Effects on the b_J- and K-band LFs at $z = 0$ of varying (a) the disk stability parameter $F_{\rm stab}$ and (b) the AGN feedback parameters $\alpha_{\rm cool}$, and (c) of turning off AGN feedback or disk instabilities, as shown by the key in each panel. A single parameter is varied in each column, with the red curves showing the standard model.

Effect of changing parameters in GALFORM

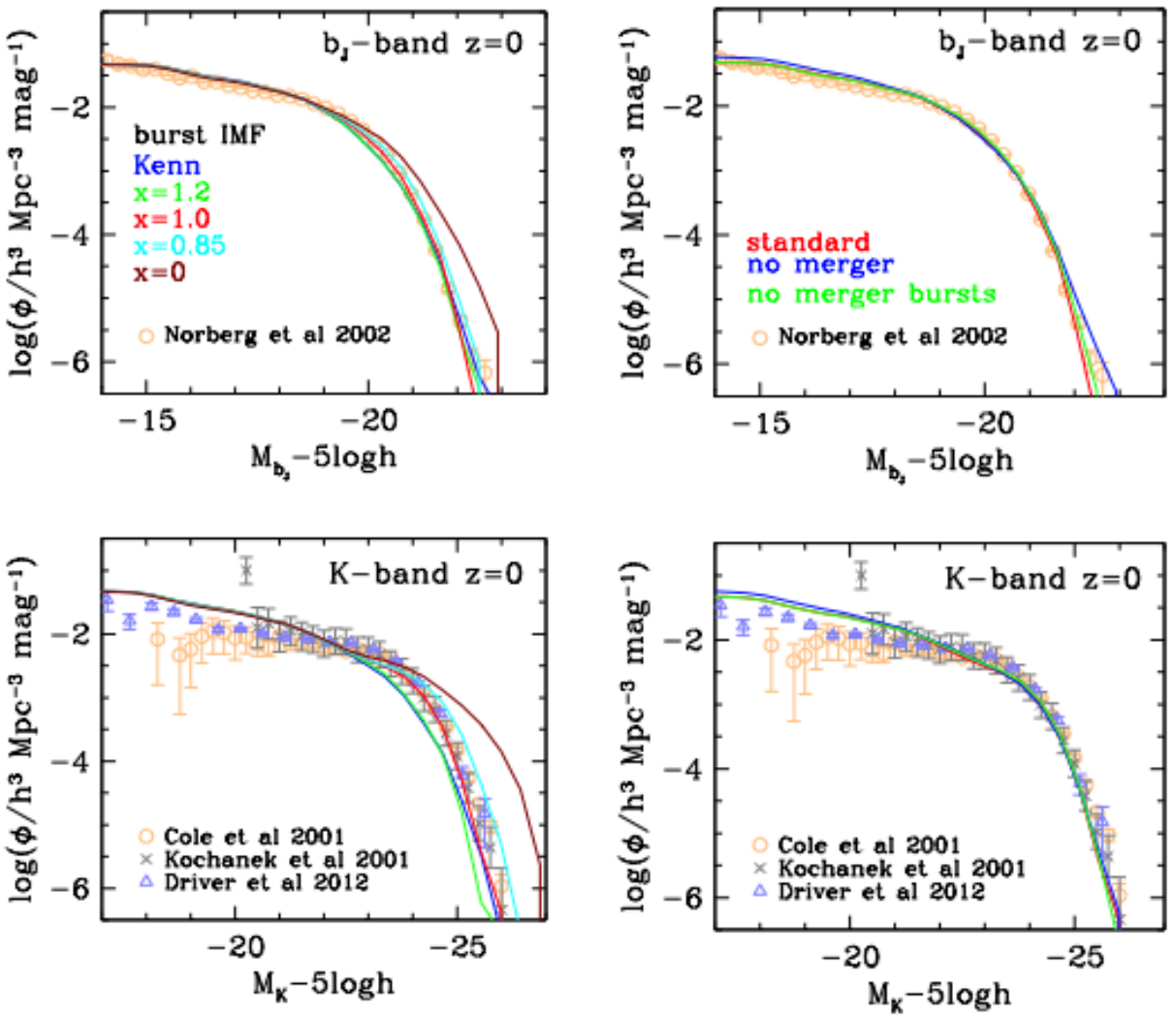

Figure C3. Effects on the b_J- and K-band LFs at $z = 0$ of (a) changing IMF in starbursts, and (b) turning off galaxy mergers or starbursts triggered by galaxy mergers, as shown by the key in each panel. A single parameter is varied in each column, with the red curves showing the standard model.

Effect of changing parameters in GALFORM

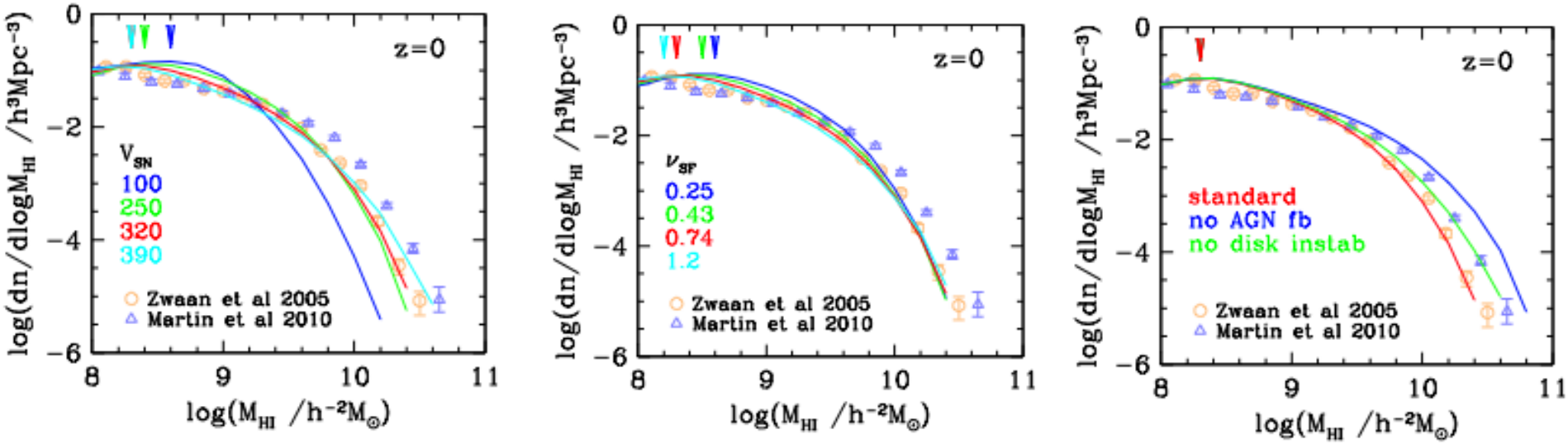

Figure C4. Effects on the HI mass function at $z = 0$ of varying (a) the strength of supernova feedback, specified by V_{SN}, and (b) the disk star formation rate, specified by ν_{SF}, and (c) of turning off AGN feedback or disk instabilities, as shown by the key in each panel. The red curves show the standard model. The vertical arrows at the top of each panel indicate the HI mass below which the results for the corresponding model are affected by the halo mass resolution. The observational data plotted are the same as in Fig. 4.

Effect of changing parameters in GALFORM

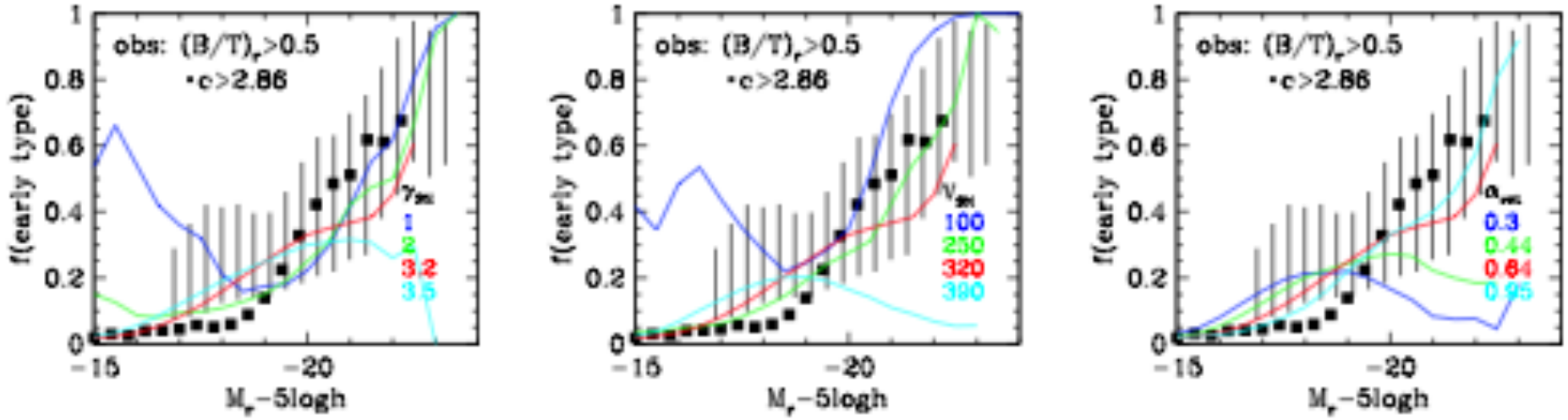

Figure C5. Effects on the fraction of early-type galaxies at $z = 0$ of varying the supernova feedback parameters $\gamma_{\rm SN}$ and $V_{\rm SN}$ and the gas return parameter $\alpha_{\rm ret}$. The red curves show the standard model. The definition of early-type galaxies in the model and the observational data plotted are the same as in Fig. 5.

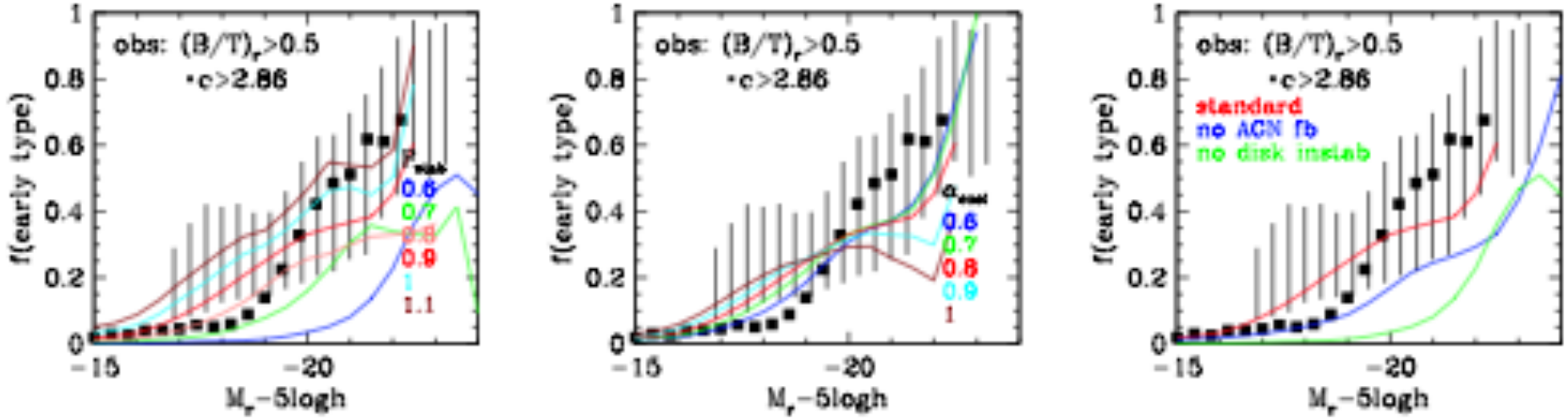

Figure C6. Effects on the fraction of early-type galaxies at $z = 0$ of varying (a) the disk stability $F_{\rm stab}$ and (b) the AGN feedback parameter $\alpha_{\rm cool}$, and (c) of turning off AGN feedback or disk instabilities. The red curves show the standard model.

Effect of changing parameters in GALFORM

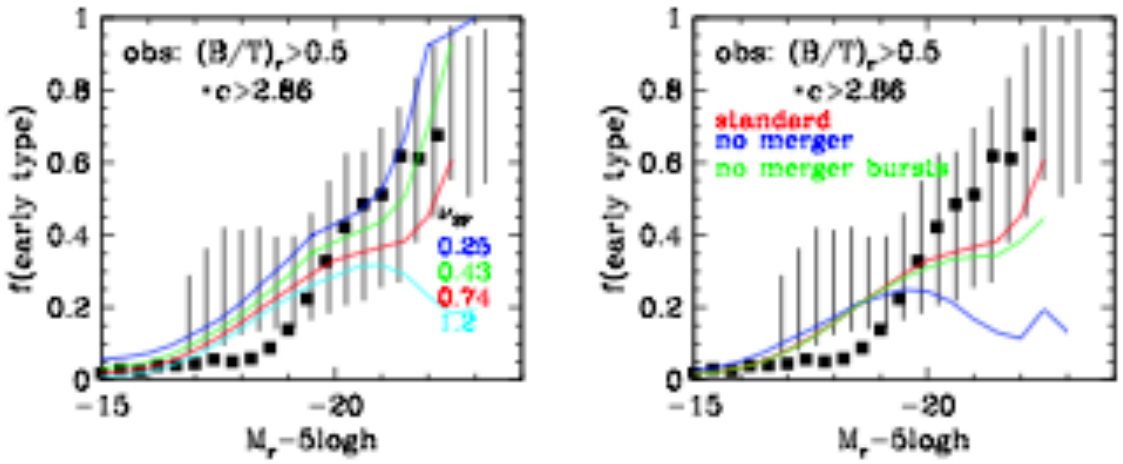

Figure C7. Effects on the fraction of early-type galaxies at $z = 0$ of (a) varying the disk star formation rate parameter ν_{SF} and (b) turning off galaxy mergers or starbursts triggered by galaxy mergers. The red curves show the standard model.

Effect of changing parameters in GALFORM

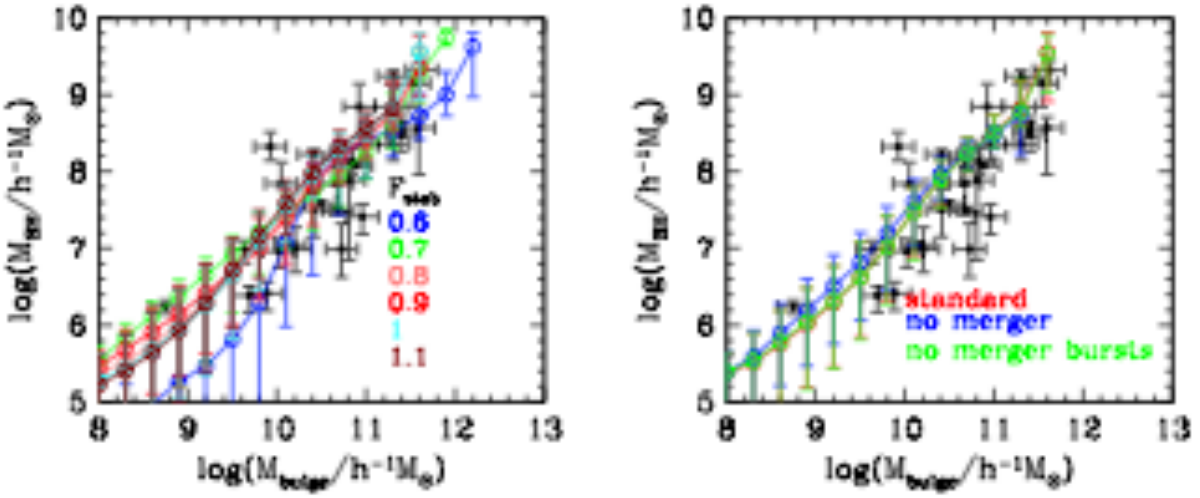

Figure C8. Effects on the SMBH - bulge relation at $z = 0$ of (a) varying the disk stability parameter $F_{\rm stab}$ and (b) turning off galaxy mergers or starbursts triggered by galaxy mergers. The red curves show the standard model. The observational data plotted are the same as in Fig. 6.

Effect of changing parameters in GALFORM

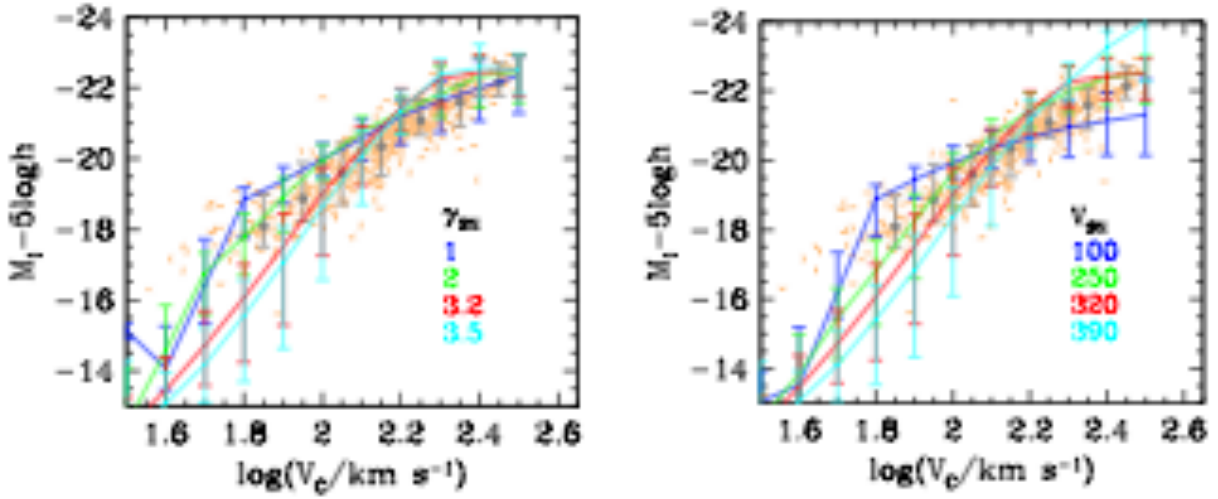

Figure C9. Effects on the I-band Tully-Fisher relation at $z = 0$ of varying the supernova feedback parameters $\gamma_{\rm SN}$ and $V_{\rm SN}$. The red curves show the standard model. The observational data plotted are the same as in Fig. 11.

Effect of changing parameters in GALFORM

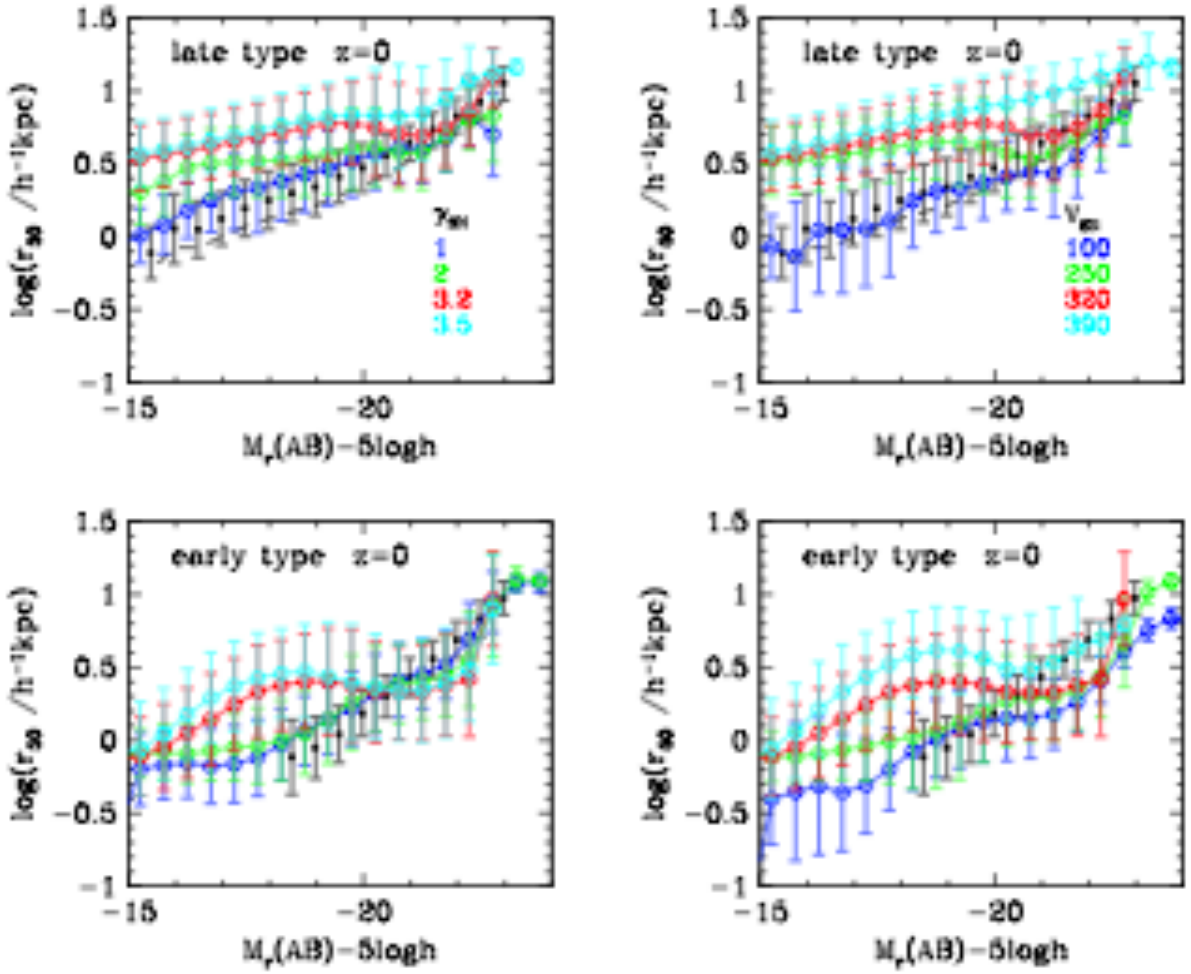

Figure C10. Effects on the half-light radii of late- and early-type galaxies at $z = 0$ of varying the supernova feedback parameters γ_{SN} and V_{SN}. A single parameter is varied in each column, with the red curves showing the standard model. The observational data plotted are the same as in Fig. 12.

Effect of changing parameters in GALFORM

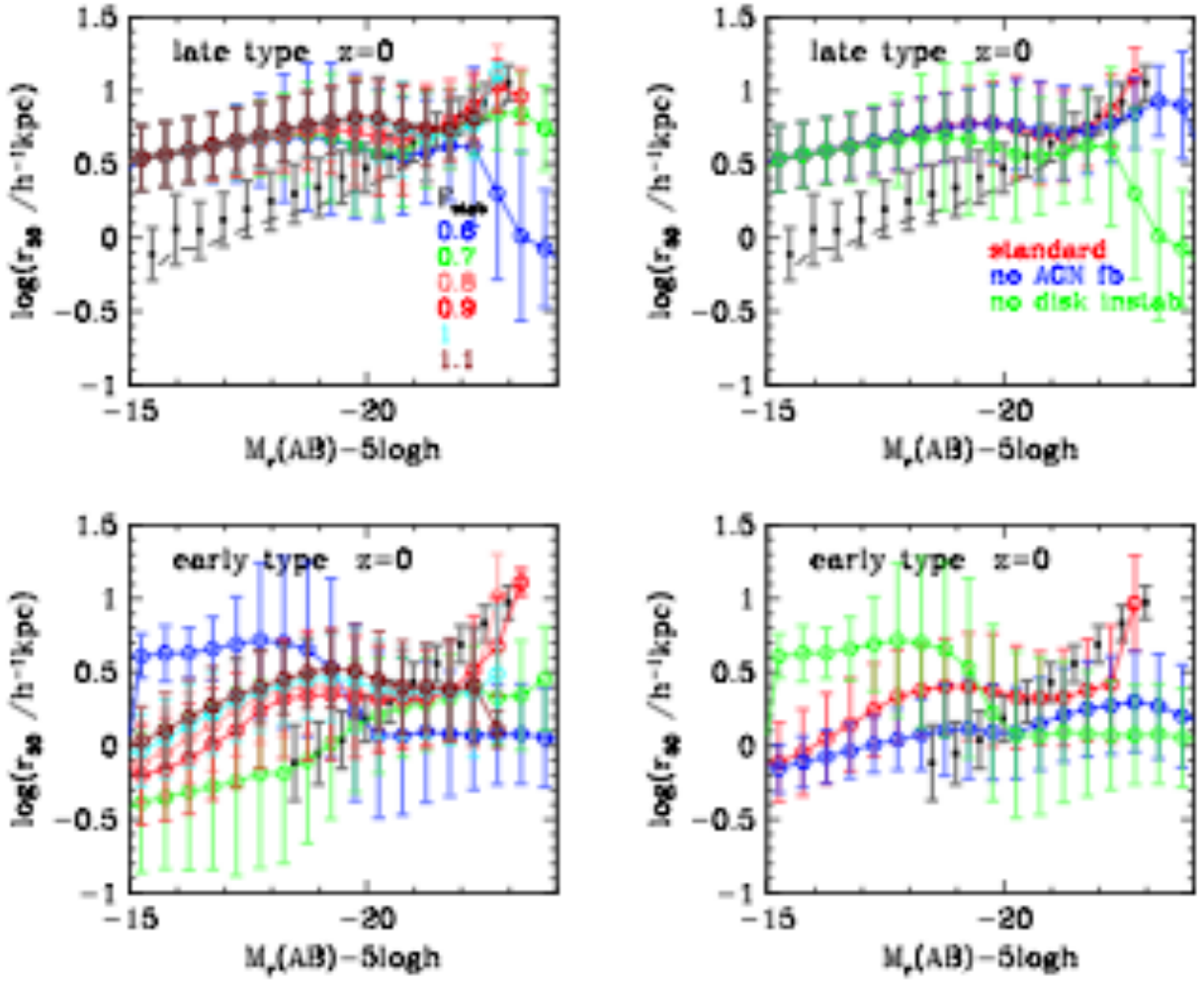

Figure C11. Effects on the half-light radii of late- and early-type galaxies at $z = 0$ of (a) varying the disk stability parameter $F_{\rm stab}$, and (b) of turning off AGN feedback or disk instabilities. A single parameter is varied in each column, with the red curves showing the standard model.

Effect of changing parameters in GALFORM

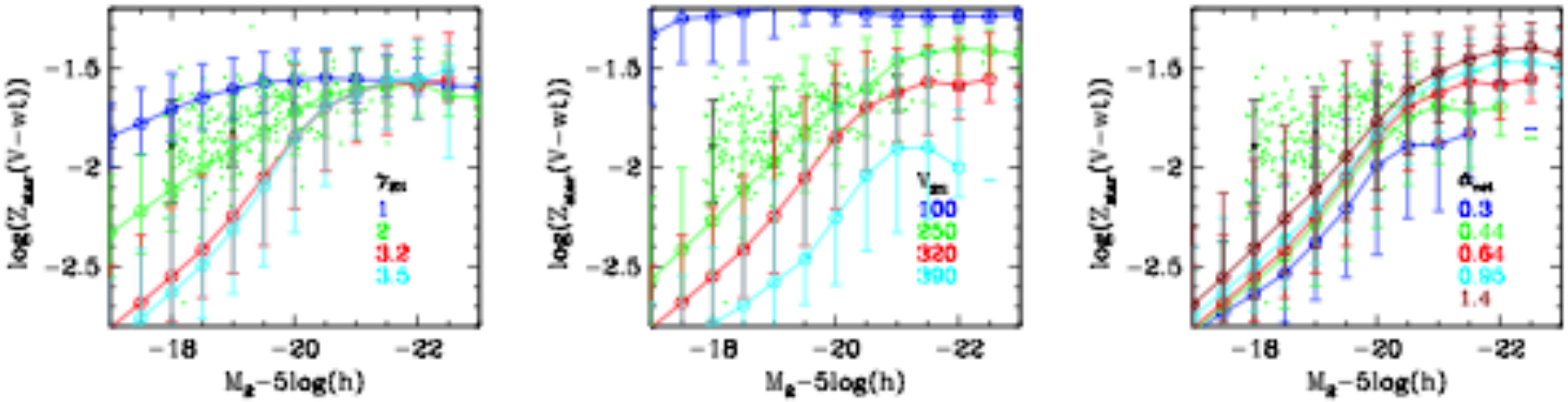

Figure C12. Effects on the stellar metallicity in early-type galaxies at $z = 0$ of varying the supernova feedback parameters $\gamma_{\rm SN}$ and $V_{\rm SN}$, and the gas return timescale parameter $\alpha_{\rm ret}$. The red curves show the standard model. The observational data plotted are the same as in Fig. 13.

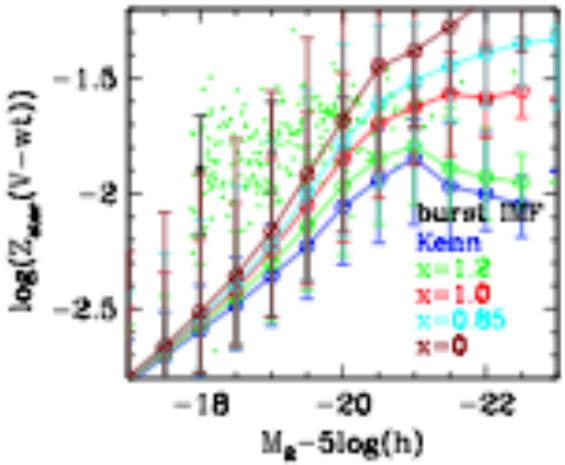

Figure C13. Effects on the stellar metallicity in early-type galaxies at $z = 0$ of changing the slope x of the starburst IMF.

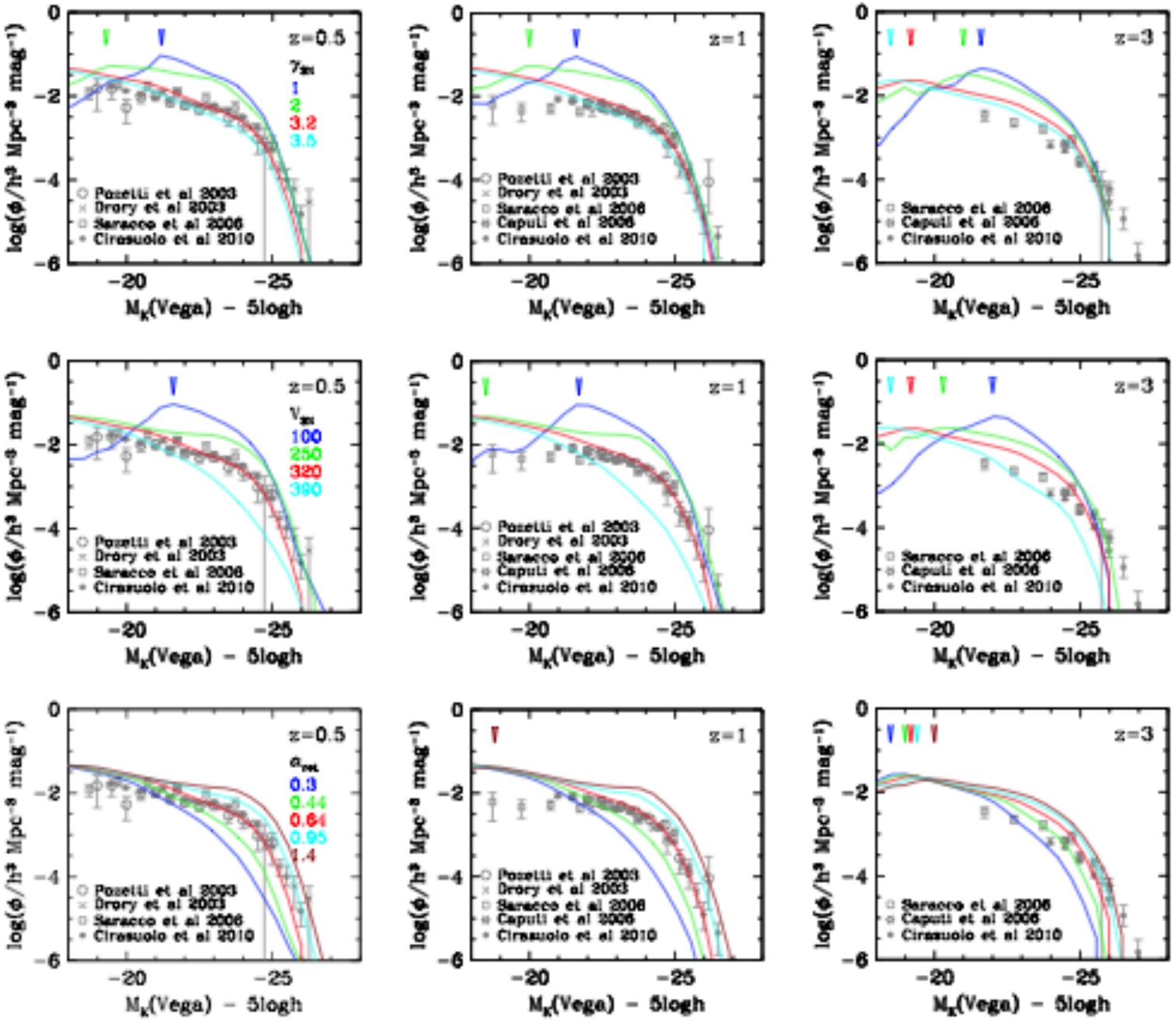

Figure C14. Effect on the evolution of the K-band luminosity function of varying the supernova feedback parameters γ_{SN} and V_{SN} and the gas return timescale parameter α_{ret}. A single parameter is varied in each row of panels, with the red curves showing the standard model. The vertical arrows at the top of each panel indicate the luminosity below which the results for the corresponding model are affected by the halo mass resolution. The observational data plotted are the same as in Fig. 7.

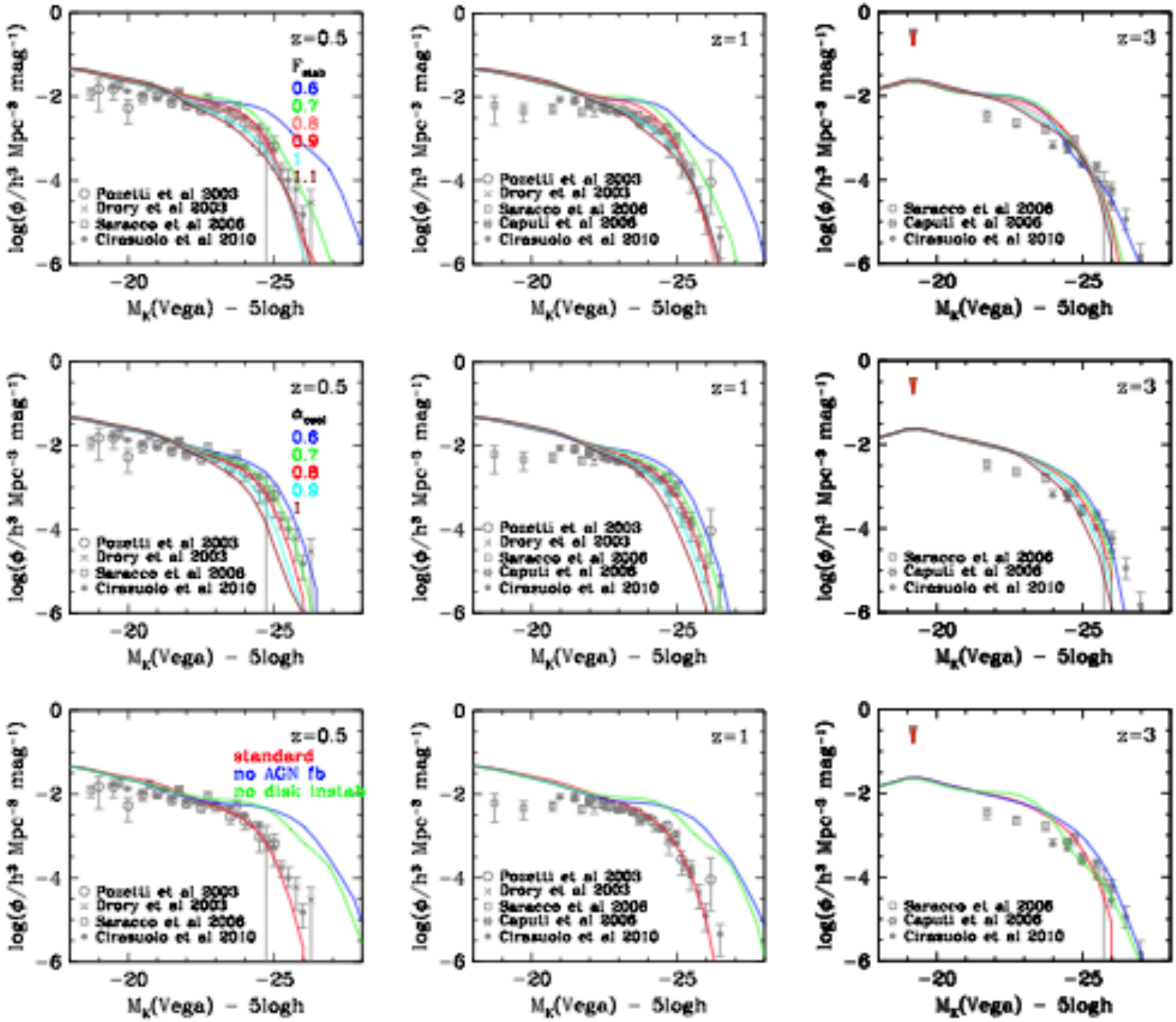

Figure C15. Effect on the evolution of the K-band luminosity function of varying (a) the disk stability parameter $F_{\rm stab}$ and (b) the AGN feedback parameter $\alpha_{\rm cool}$, and (c) of turning off AGN feedback or disk instabilities. A single parameter is varied in each row of panels, with the red curves showing the standard model.

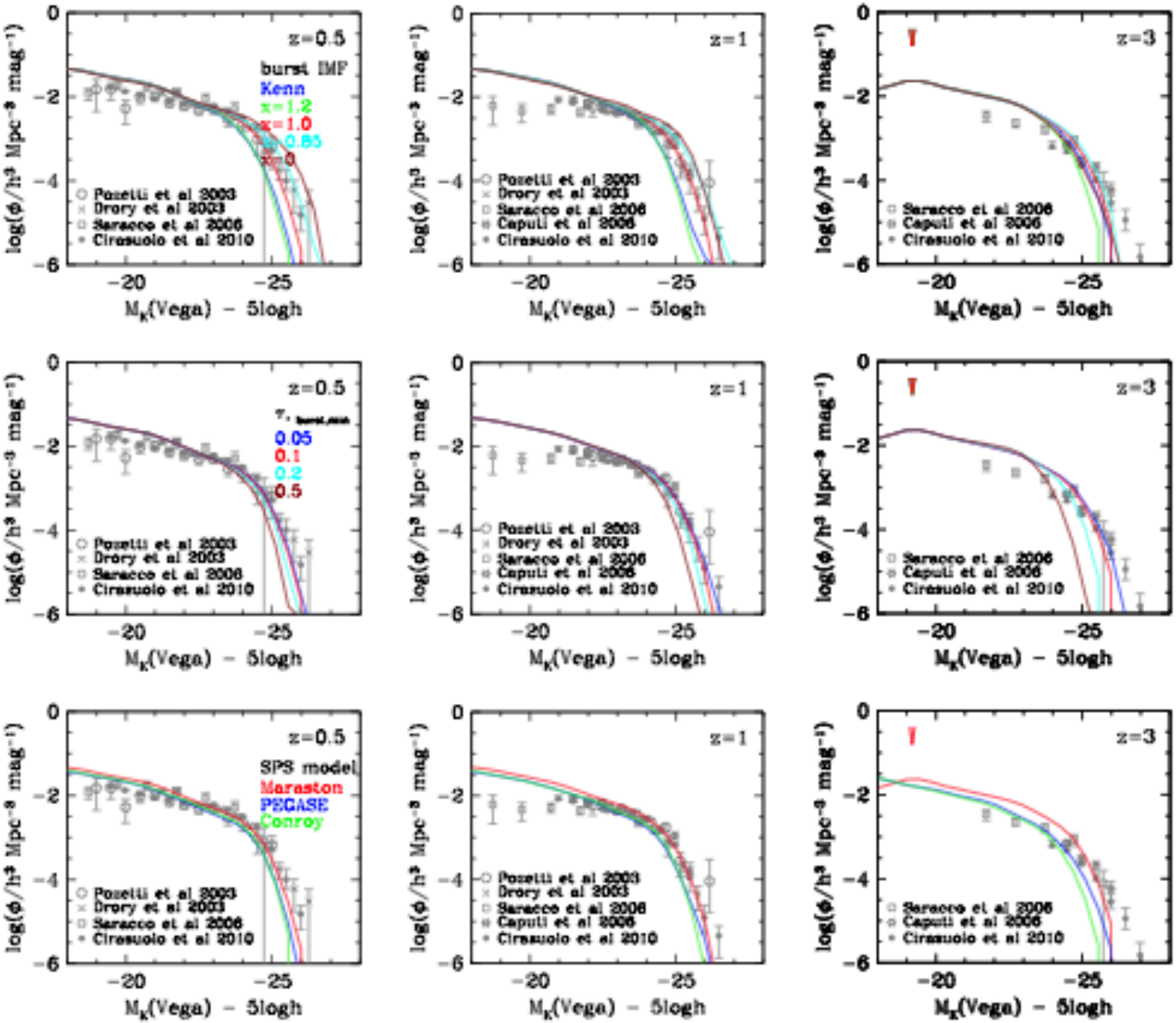

Figure C16. Effect on the evolution of the K-band luminosity function of varying (a) the slope x of the starburst IMF, (b) the minimum starburst timescale $\tau_{*\mathrm{burst,min}}$ and (c) the SPS model. A single parameter is varied in each row of panels, with the red curves showing the standard model.